Effect of protein shape on multibody interactions between membrane inclusions

K. S. Kim,[1,*] John Neu,[2] and George Oster[3,†]
[1]*Department of Physics, Graduate Group in Theoretical Biophysics, University of California, Berkeley, California 94720*
[2]*Department of Mathematics, University of California, Berkeley, California 94720*
[3]*Department of Molecular and Cellular Biology, University of California, Berkeley, California 94720*
(Received 15 July 1999; manuscript received revised 19 November 1999)

The elastic interaction of membrane inclusions provides one of the simplest physical realizations of multibody forces. Here we show how the cross-sectional shape of the inclusion greatly changes the character of the interaction, and illustrates a pattern formation mechanism. The formalism provides a transparent framework for modeling bilayer-inclusion boundary effects on the multibody interaction.

PACS number(s): 87.15.Kg, 87.18.Hf, 68.10.Et, 87.16.Dg

There has been a great deal of interest and work on bilayer-mediated forces between membrane proteins (inclusions) [1–6]. Here we address interactions that are induced by elastic deformations, since they are thought to play an important role in the aggregation of membrane proteins [7–10]. An embedded inclusion creates a deformation field in the surrounding membrane that influences neighboring inclusions. The nature of this deformation field is dictated by the inclusions's elasticity and shape, and by the elastic properties of the membrane. In an earlier paper [7], we examined the deformation field generated by circularly symmetric inclusions embedded in a membrane whose elastic energy is determined by its curvature. We found that the interaction between $N>2$ inclusions was nonlinear and strongly nonpairwise. Therefore, simple pairwise theories of inclusion aggregation driven by membrane curvature cannot accurately describe assemblies of inclusions. This led to the surprising result that aggregates relax to stable equilibria even though the pairwise component of the interaction is repulsive. Here we generalize the theory to inclusions whose cross-sectional shapes are not circular. The orientation angles of the inclusions appear as additional degrees of freedom which add to the complexity of possible spatial patterns. We will explicitly derive a multibody interaction that provides a simple framework for studying how inclusion geometry (cross-sectional shape) coupled with membrane geometry (curvature) can lead to interesting and unusual aggregation behavior.

Our derivation of the interaction energy begins by representing a membrane, as a surface **S**, parametrized by the height, h, above the (x, y) plane. The projection of **S** onto the (x, y) plane is denoted by **s**. Denote points in **S** by **X**, and points in **s** by $\mathbf{x}=(x_1,x_2)$. Unit vectors in the coordinate directions are denoted (**1**, **2**, **3**). Our notation is summarized in Fig. 1. We will restrict our attention to a membrane system consisting of rigid inclusions whose contact curve with the membrane, **C**, is an ellipse, and the tangent planes of **S** along **C** have a uniform contact angle, γ. The same mathematical formalism and results derived here will also apply for inclusions with undulating bilayer-inclusion contact curve, since the boundary conditions will have essentially the same form. This can be physically realized when an inclusion consists of different subunits with different contact angles for the bilayer, as shown in Fig. 1(b). In both cases there will be an orientation dependent interaction term in the energy, which will generate a torque on the inclusion tending to orient itself so that the inclusion-bilayer contact curve matches as closely as possible to the local shape of the membrane background.

In the small deformation limit, $|\nabla h(\mathbf{x})|\ll 1$, the local mean curvature of **S** at $\mathbf{X}=\mathbf{x}+\mathbf{z3}$ is $\kappa(\mathbf{x})\equiv\frac{1}{2}\nabla^2 h(\mathbf{x})$. The elastic bending energy for a membrane is given by [11]

$$E_m(\mathbf{X})=\frac{B}{2}\int_{\mathbf{S}}[\nabla^2 h(\mathbf{x})]^2 d\mathbf{x}=2B\int_{\mathbf{S}}\kappa^2 d\mathbf{x}, \qquad (1)$$

where B is the bending modulus. We neglect the total Gaussian curvature term since it plays no role in the interaction between rigid inclusions. Admissible inclusion configurations are determined by a constrained minimization of the energy (1). In the variational calculation, variations of the displacement field, h, cannot assume arbitrary values along the projected contact curves, **c**. The variations must be consistent with rigid body motions of the contact curves, **C**, and tangent planes along **C**. The variational equations consist of the biharmonic equation for h

$$\nabla^4 h=0 \quad \text{in } \mathbf{S}, \qquad (2)$$

and vector-valued integral constraints that represent the balances of forces and torques in the inclusions [7]. In the small deflection limit, imbalances of vertical forces and horizontal torques carry by far the largest energy penalties; thus one expects a rapid relaxation to configurations in which vertical forces and horizontal torques balance. The energies of these restricted configurations are determined uniquely by the configuration of projected contact curves, **c**. Therefore, there is an effective multibody energy that depends on the configuration of projected contact curves, **c**, and it determines the remaining horizontal forces and vertical torques. What now follows is an approximate calculation of this multibody energy for a system of noncircular inclusions.

*Electronic address: kkim@nature.berkeley.edu
†Electronic address: goster@nature.berkeley.edu

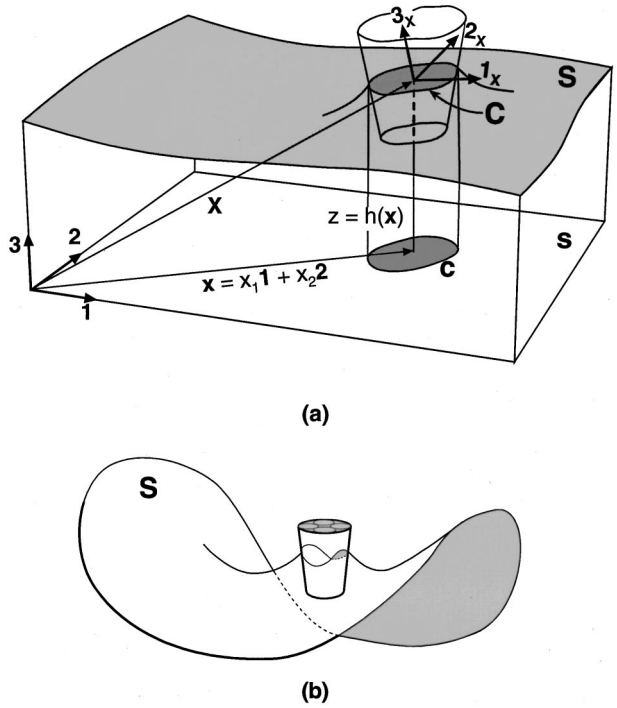

FIG. 1. (a) The membrane coordinate representation defining the various quantities used in the text. (b) An undulating inclusion-bilayer contact curve that gives the same energy as an inclusion with an elliptic cross section.

We restrict our attention to inclusions whose elliptical cross-sectional shape is a small perturbation of a unit circle, and which are widely spaced compared to their diameter. Under these conditions there are finite energy configurations in which the mean curvature energy is concentrated in annuli of thickness unity about the inclusions. The analysis of these energy concentrations for circular inclusions was presented in Ref. [7]. We generalize that analysis to elliptical inclusions. As in Ref. [7], the mean curvature field in the neighborhood of an inclusion centered about $r=0$ is approximated to leading order by the quadrupole field

$$\kappa=\frac{1}{r^2}(a_2\cos 2\theta+b_2\sin 2\theta). \tag{3}$$

This quadrupole field is harmonic, as required by the biharmonic equation for h, and is square integrable, which means that there is a finite amount of mean curvature energy concentrated about the inclusion. In fact, the total energy concentrated about the inclusion is approximated to leading order by

$$E=\pi B(a_2^2+b_2^2). \tag{4}$$

The quadrupole coefficients a_2,b_2 in Eq. (3) are determined by the position and orientations of the other inclusions far from $r=0$. This determination is simplest to understand by first considering the displacement field $h=\phi(\mathbf{x})$ in a neighborhood of $r=0$ with the inclusion about $r=0$ absent, and then analyzing the perturbation when the inclusion is inserted into the membrane. The background field $\phi(\mathbf{x})$ is given to leading order by a quadratic harmonic function, $\phi\approx\alpha/2(x_1^2-x_2^2)+\beta x_1x_2$, where $\alpha\equiv\partial_{11}\phi(\mathbf{0})=-\partial_{22}\phi(\mathbf{0})$, $\beta\equiv\partial_{12}\phi(\mathbf{0})$.

This approximation to ϕ holds for r much smaller than interinclusion distance. With the inclusion about $r=0$ present, the leading order displacement field now takes the form

$$h=-\gamma\ln r+\left(\frac{\alpha}{2}r^2+\frac{\alpha_2}{r^2}-\frac{a_2}{2}\right)\cos 2\theta+\left(\frac{\beta}{2}r^2+\frac{\beta_2}{r^2}-\frac{b_2}{2}\right)\sin 2\theta. \tag{5}$$

Here α,β are the coefficients associated with the background field $\phi(\mathbf{x})$, and as such, are assumed given. The coefficients α_2,β_2 and a_2,b_2 are to be determined from inclusion-bilayer contact boundary conditions. Given the determination of a_2,b_2, the energy (4) can be calculated. Equation (5) represents the most general biharmonic displacement field with quadrupole symmetry which has associated mean curvature field (3) and exhibits asymptotic matching with the background field $\phi(\mathbf{x})$ for $1\ll r\ll$ interinclusion distance.

Next, we formulate and outline the determination of a_2,b_2. The contact curve is represented by the ellipse $r(\theta)=1+\varepsilon\cos(\theta-\omega)$; $0\ll\varepsilon\ll 1$ is the small eccentricity and ω represents the angle between the major axis and the unit vector $\mathbf{1}$. A natural generalization of the above parametrization is a ''scalloped'' contact curve given by $r=1+\varepsilon\cos[n(\theta-\omega)]$ where n is an integer greater than 3. Treatment of ''scalloped'' inclusions requires higher order multipole terms in the formulas (3), (5) for mean curvature and displacement, and there are collateral modifications of the energy (4). For elliptical contact curves, the boundary conditions are

$$h[1+\varepsilon\cos 2(\theta-\omega)]=0,\qquad h_r[1+\varepsilon\cos 2(\theta-\omega)]=-\gamma. \tag{6}$$

These reduce to the boundary conditions for a circular inclusion when $r=1$.

For small eccentricity, ε, one can Taylor expand and obtain effective boundary conditions at $r=1$. We will also assume that the solution is a small perturbation from the leading term $-\gamma\ln(r)$ in Eq. (5). Thus we obtain the following effective boundary conditions:

$$h(1,\theta)=\varepsilon\gamma\cos 2(\theta-\omega)+O(\varepsilon^2),\qquad h_r(1,\theta)=-\gamma-\varepsilon\gamma\cos 2(\theta-\omega)+O(\varepsilon^2). \tag{7}$$

With these boundary conditions, we can now determine the coefficients of the displacement field (5). In particular, the coefficients a_2 and b_2 which appear in the energy (4) are

$$a_2=2\alpha-\varepsilon\gamma\cos 2\omega,\qquad b_2=2\beta-\varepsilon\gamma\sin 2\omega. \tag{8}$$

It will be useful to introduce the following complex notation. Define a complex curvature scalar as $\eta=\alpha-i\beta$ and the elip-

ticity scalar as: $\zeta \equiv (\varepsilon\gamma/2)e^{-i2\omega}$. The energy formula (4) with a_2, b_2 given by Eq. (8) can be summarized as

$$E = \pi B |\eta - \zeta|^2. \tag{9}$$

We can think of Eq. (9) as the ''energy cost for introducing an inclusion into a background curvature η.'' Note that for $\varepsilon = 0$, Eq. (9) reduces to the expression derived earlier for circular inclusions [7].

Suppose that the background field, ϕ, is due to $N-1$ proteins far from the origin. It is convenient to represent positions in the base plane by complex variables z, and inclusion positions by z_i, $i = 2,...,N$. The leading order harmonic component of ϕ seen in the neighborhood of the origin is given by $\phi \approx -\gamma \Sigma_{i=2}^{N} \ln|z - z_i|$. Hence, the curvature scalar is given by $\eta = \alpha - i\beta = \Sigma_{i=1}^{N} (\gamma / z_i^2)$. Therefore, the energy cost (9) of inserting a protein at the origin into the background curvature generated by all the other inclusions is given by $E = \pi B |\gamma \Sigma_{i=2}^{N} (1/z_i^2) - \zeta|^2$. The total multibody interaction energy between N inclusions at positions z_i, $i = 1,...,N$ with ellipticity scalars ζ_i is given by

$$E = \pi B \sum_j \left| \gamma \sum_{i \neq j} \frac{1}{(z_j - z_i)^2} - \zeta_j \right|^2. \tag{10}$$

From Eq. (10), we see that the energy of a pair of inclusions is

$$E = \pi B \left(\left| \frac{\gamma}{z^2} - \zeta_1 \right|^2 + \left| \frac{\gamma}{z^2} - \zeta_2 \right|^2 \right), \tag{11}$$

where z represents the displacement between the inclusions. We can determine the relative orientations of the two inclusions by observing that the minimum energy of zero is attained when $\zeta_1 = \zeta_2 = \gamma / z^2$, where the subscripts refer to inclusion 1 and 2. These complex identities define a one parameter family of zero energy configurations, $z = \sqrt{2/\varepsilon}\, \exp(i\omega)$, where $\omega_1 = \omega_2 = \omega$ is arbitrary. The existence of a family of zero energy states also follows from rotational symmetry. At the zero energy configuration, the two inclusions will be separated by a characteristic separation of $r = \sqrt{2/\varepsilon}$, and will be oriented such that the major axes of both inclusions are collinear. Any other pair of orientations will have higher energy. Figure 2 shows the energy surface of the two inclusions as a function of their individual orientations ω_1 and ω_2 at a fixed relative distance. The three stationary points of the energy surface correspond to the three relative orientations of the inclusions depicted in Fig. 2. The global minimum of zero energy occurs when the major axes are collinear: $\omega_1 = \omega_2 = 0$. The global maximum occurs when the major axes are parallel: $\omega_1 = \omega_2 = \pi/2$, which is an unstable configuration. The energy surface has a saddle point when the inclusions are mutually perpendicular in a T configuration: $\omega_1 = 0$, $\omega_2 = \pi/2$, and vice versa.

We can get a better physical picture of this interaction by considering a single inclusion interacting with a given membrane curvature, defined by the complex scalar η. The energy (9) is minimum when the elliptical scalar ζ is proportional to the curvature scalar η. Geometrically this means that the elliptical inclusion aligns its major axis so as to match as closely as possible the local shape of the background curvature field. This background field can be characterized locally by its principal axes. Consider a single pair of identical inclusions separated by a distance r. Assuming proper alignment of the elliptical scalars, the total interaction energy of the pair is: $E = 2\pi B[(\gamma/r^2) - (\varepsilon\gamma/2)]^2$. A plot of the energy as a function of separation is shown in the inset in Fig. 2. Note that if $\varepsilon = 0$, we obtain the repulsive pair potential between two circular inclusions derived in Ref. [7]: $E = 2\pi B \gamma^2 / r^4$.

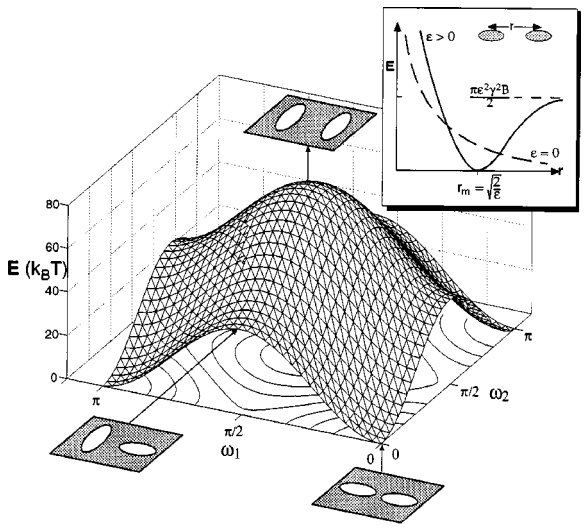

FIG. 2. The energy surface for two inclusions as a function of their individual orientations, ω_1 and ω_2. Inset: The interaction energy between a pair of inclusions as a function of separation, r.

The character of the interaction is fundamentally different when the ellipticity parameter $\varepsilon > 0$. As seen from Fig. 2 (inset), the interaction between a pair becomes attractive for $r > \sqrt{2/\varepsilon}$ and repulsive for $r < \sqrt{2/\varepsilon}$. The energy achieves a global minimum of zero at separation $r = \sqrt{2/\varepsilon}$.

In systems of $N > 2$ inclusions there will be a complicated interplay between the nonpairwise interactions and inclusion orientations. The simplest system in which this occurs is for $N = 3$. Consider three identical elliptical inclusions arranged at the vertices of an equilateral triangle with sides $r = \sqrt{2/\varepsilon}$ and with orientations $(z = 0, \omega = \pi/6)$, $(z = r, \omega = 5\pi/6)$, and $(z = re^{i\pi/3}, \omega = \pi/2)$. The curvature scalar at $z = 0$ due to the other two inclusions is $\eta = (\gamma/r^2) + (\gamma/r^2 e^{i2\pi/3}) = (\gamma/r^2)e^{i\pi/3}$. Therefore, the inclusion at $z = 0$ contributes energy $\pi B[(\gamma/r^2) - (\varepsilon\gamma/2)]^2$; the energy due to each of the remaining two inclusions is the same by symmetry. The total energy is then $E = 3\pi B[(\gamma/r^2) - (\varepsilon\gamma/2)]^2$. The energy achieves its minimum value of zero at $r = \sqrt{2/\varepsilon} = r_b$, so that this configuration of three inclusions is stable. From the energy formula, we can deduce that a system whose initial configuration is an equilateral triangle with the above orientations and whose sides are greater than this length scale will uniformly shrink until it reaches the characteristic size of r_b. This is dramatically different than for circular symmetric inclusions, where the smallest stable aggregate was $N = 5$ inclusions arranged in the vertices of a regular pentagon [7].

We see that in introducing an additional degree of freedom (inclusion orientation) to the many-body interaction, the form of the potential energy has qualitatively changed its character from a $1/r^4$ repulsion to an $1/r^2$ attraction. This has

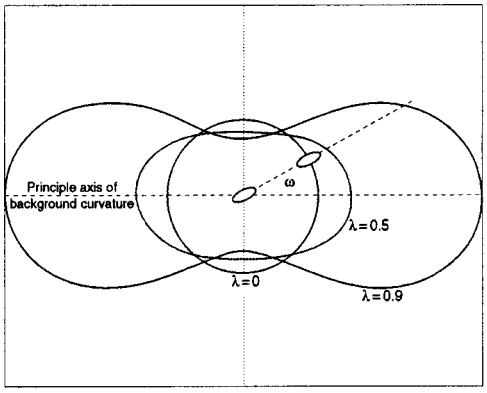

FIG. 3. One parameter family of zero energy configurations of a bound pair in a background field of distant proteins, parametrized by $\lambda \equiv (\eta_b/\varepsilon\gamma/2)$. The horizontal axis is placed along the principal axis of the background curvature which is concave upwards.

important consequences with regards to protein aggregation. From the above simple examples of $N=2$ and $N=3$ inclusions, one can predict the position and orientation patterns of a stable aggregate of inclusions. Within our formalism, one can further analyze higher harmonics of the shape function, and derive other interactions which will generate new patterns of inclusion aggregates. We do not yet know whether such analysis will reveal an inverse mapping from known equilibrium patterns to unknown inclusion shapes.

We can get a picture of what happens for $N>3$ by examining a special case. Another striking manifestation of nonpairwise forces arises when we consider a bound pair of inclusions in a background field of distant inclusions. Consider again a single inclusion pair. If this pair were placed in a background field of distant inclusions, the energy of the pair will be

$$E = \pi B \left\{ \left| \frac{\gamma}{z^2} + \eta_b - \zeta_1 \right|^2 + \left| \frac{\gamma}{z^2} + \eta_b - \zeta_2 \right|^2 \right\}, \qquad (12)$$

where η_b is the curvature scalar of the background field. It is convenient to assume that coordinate axes **1**,**2** coincide with the principal axes of the quadratic background field $\phi(\mathbf{x})$. In this case, η_b is real. If the background inclusions are far away from the target pair, we can assume that the background curvature is uniform over the region occupied by the pair. As in the previous example of a single isolated pair of inclusions, we can determine a one parameter family of zero energy configurations: $z = \sqrt{2/\varepsilon}\exp(i\omega)/\sqrt{1-(2\eta_b/\varepsilon\gamma)\exp(i2\omega)}$. As before, the free parameter ω is the common orientation angle for major axis of both inclusions relative to the **1** axis. Note that this expression agrees with the result for an isolated pair of inclusions when the background curvature $\eta_b \to 0$. The interesting feature here is that the one parameter family of zero energy states persists even in the presence of far field background curvature $\eta_b \neq 0$. Figure 3 is a plot of the zero energy contours for various η_b in the ratio $\lambda \equiv \eta_b/(\varepsilon\gamma/2)$. $\lambda = 0$ represents a single isolated pair of inclusions. The angle ω is with respect to one of the principal axes represented in the figure as the horizontal axis. Recall that the background curvature field sets the principal axes at any given local point of the membrane.

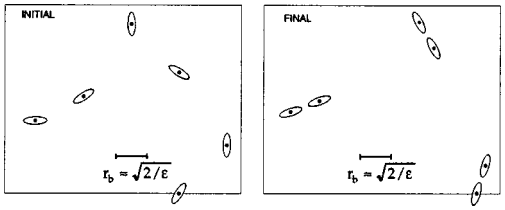

FIG. 4. (a) Initial configuration of six inclusions. (b) Final configuration of three bound pairs.

Another interesting result displayed in Fig. 3 is the fact that as the background curvature, η_b, increases, the zero energy curve and thus the ground state degeneracy increases in size. In a companion paper, we will show that, at finite temperatures, this increase of zero energy leads to an entropic attraction between pairs.

From this analysis, a bound pair at its zero energy state can persist in a background of distant inclusions. This suggests the following scenario. Given an initial configuration of inclusions distributed in such a way that any one inclusion has a unique nearest neighbor and thereby treating the others as a background field, the above analysis predicts a final equilibrium configuration consisting of islands of bound pairs. Within each pair, the inclusions will be oriented collinearly, with their major axes parallel. We can follow the evolution of a field of inclusions by solving the gradient flow system, $\zeta d\mathbf{x}/dt = -\nabla E(\mathbf{x})$, where $E(\mathbf{x})$ is the multibody energy (10). Figure 4(a) shows a simulation of a system of six inclusions with the above initial conditions but otherwise randomly distributed in position and orientation. The final equilibrium configuration shown in Fig. 4(b) consists of three bound pairs of inclusions, each with its aligned orientation and characteristic separation r_b, in agreement with predictions. Each bound pair interacts very weakly with other bound pairs, unless they are within the distance of their characteristic separation. Within this distance, nonpairwise effects will become important, and one can further analyze whether the pairs would coalesce and form bound triplets or quartets, and so on.

Other interesting final configurations consistent with this result are a chain of inclusions whose orientations are slowly varying with the length of the chain. For generic N-body simulations, we have found many configurations which correspond to extremal states which may be metastable to small perturbations. Therefore, the final configuration generally depends on the initial conditions. We have already encountered such a problem when we examined the energy surface of two inclusions as a function of their orientations. Superimposed on this energy surface is the complicated multidimensional energy surface due to nonpairwise curvature interactions. As the number of inclusions increases it becomes more difficult to determine which among these extremal configurations are the true stable equilibria. In a companion paper, we will introduce finite temperature effects [12]. There we will show that incorporating thermal fluctuations effects in the interparticle displacements and orientations can break this degeneracy.

ACKNOWLEDGMENTS

K.K. and G.O. were supported by the NSF through Grant No. DMS 9220719.

[1] S. Marcelja, Biophys. J. **76**, 593 (1999).
[2] R. S. Cantor, Biophys. J. **76**, 2625 (1999).
[3] R. S. Cantor, Toxicology Letters **100-101**, 451 (1998).
[4] N. Dan and S. A. Safran, Biophys. J. **75**, 1410 (1998).
[5] S. May and A. Ben-Shaul, Biophys. J. **76**, 751 (1999).
[6] H. Arando-Espinoza *et al.*, Biophys. J. **71**, 648 (1996).
[7] K. S. Kim, J. Neu, and G. Oster, Biophys. J. **75**, 2274 (1998).
[8] M. Goulian, R. Bruinsma, and P. Pincus, Europhys. Lett. **22**, 145 (1993).
[9] N. Dan, P. Pincus, and S. A. Safran, Langmuir **9**, 2768 (1993).
[10] J. M. Park and T. C. Lubensky, J. Phys. I **16**, 1217 (1996).
[11] W. Helfrich, Z. Naturforsch. C **28**, 693 (1973).
[12] T. Chou, K. Kim, and G. Oster (unpublished).